THE JOURNAL OF BIOLOGICAL CHEMISTRY VOL. 286, NO. 37, pp. 32661–32671, September 16, 2011

Arrested Oocyst Maturation in *Plasmodium* Parasites Lacking Type II NADH:Ubiquinone Dehydrogenase*[S]

Received for publication, June 20, 2011, and in revised form, July 18, 2011 Published, JBC Papers in Press, July 19, 2011, DOI 10.1074/jbc.M111.269399

Katja E. Boysen and Kai Matuschewski[1]

From the Parasitology Unit, Max Planck Institute for Infection Biology, 10117 Berlin, Germany

The *Plasmodium* mitochondrial electron transport chain has received considerable attention as a potential target for new antimalarial drugs. Atovaquone, a potent inhibitor of *Plasmodium* cytochrome bc_1, in combination with proguanil is recommended for chemoprophylaxis and treatment of malaria. The type II NADH:ubiquinone oxidoreductase (NDH2) is considered an attractive drug target, as its inhibition is thought to lead to the arrest of the mitochondrial electron transport chain and, as a consequence, pyrimidine biosynthesis, an essential pathway for the parasite. Using the rodent malaria parasite *Plasmodium berghei* as an *in vivo* infection model, we studied the role of *NDH2* during *Plasmodium* life cycle progression. *NDH2* can be deleted by targeted gene disruption and, thus, is dispensable for the pathogenic asexual blood stages, disproving the candidacy for an anti-malarial drug target. After transmission to the insect vector, NDH2-deficient ookinetes display an intact mitochondrial membrane potential. However, *ndh2*(−) parasites fail to develop into mature oocysts in the mosquito midgut. We propose that *Plasmodium* blood stage parasites rely on glycolysis as the main ATP generating process, whereas in the invertebrate vector, a glucose-deprived environment, the malaria parasite is dependent on an intact mitochondrial respiratory chain.

Apicomplexan parasites of the genus *Plasmodium* are the causative agents of malaria. Worldwide, malaria accounts for >200 million infections and nearly 1 million deaths every year (1). The emergence and ongoing spread of resistance to antimalarial drugs calls for the development of new antimalarial compounds (2). Cases of resistance to almost all quinolone and antifolate drugs have been reported as well as decreased susceptibility to artemisinin drugs (3).

The *Plasmodium* mitochondrial electron transport chain (mtETC)[2] is a validated target for the development of antimalarial drugs (4–6). The effects of atovaquone on cytochrome bc_1 (7) and candidate inhibitors on dihydroorotate dehydrogenase (DHOD) (8–11), succinate dehydrogenase (12, 13), and the NADH:ubiquinone oxidoreductase (NDH2) (14–19) have been studied. However, the *in vivo* functions and physiological relevance of the mtETC components are still not understood.

In *Plasmodium* parasites NDH2 is one of five mitochondrial dehydrogenases that feed electrons into the mtETC (Fig. 1). Typically, eukaryotes possess a multicomponent rotenone-sensitive NADH:ubiquinone oxidoreductase, also termed complex I, which is located in the inner mitochondrial membrane. It catalyzes the transfer of electrons from NADH to ubiquinone (coenzyme Q (Q)) leading to the reduced form, ubiquinol (QH_2), and is involved in establishing the electropotential across the inner mitochondrial membrane ($\Delta\psi_m$) by pumping hydrogen ions out of the mitochondrial matrix (20, 21). *Plasmodium* spp., however, has a rotenone-insensitive, single subunit NADH:quinone oxidoreductase, also termed alternative complex I or NDH2 (22). This enzyme is found in some bacteria and archaea as well as in yeast and plants (23). It is characterized by the lack of a transmembrane domain, by conserved triglyceride nucleotide binding motifs (G*X*G*XX*G), and by the apparent lack of any detectable proton pump activity. Although in general NDH2 sequences are highly divergent, this protein is relatively well conserved among *Plasmodium* species (supplemental Fig. 1). Structural information remains elusive, but a first prediction of a *Plasmodium falciparum* NDH2 structure has been proposed based on sequence and similarity data (14, 19, 24). Sensitivity of *P. falciparum* NDH2 to various inhibitors, such as dibenziodolium chloride (CID 16219231), diphenyliodonium chloride (CID 73870), and the quinolone derivative HDQ (2-dodecylquinolin-4-ol,1-oxide; CID 600305), has been reported (25). However, the drugs proved to be neither effective nor specific for NDH2 (19, 26, 27).

The electron transfer from NADH to Q has been shown to follow a ping-pong mechanism, possibly to maintain a pool of oxidized NADH, which in turn can be used for metabolic processes, such as glycolysis (28). At the same time, NDH2 feeds electrons into the mtETC, thereby contributing indirectly to the $\Delta\psi_m$. However, the relevance of the plasmodial *NDH2* as well as of the mtETC and the mitochondrial membrane potential *in vivo*, in particular throughout the *Plasmodium* life cycle, is not yet elucidated. In other eukaryotes, one of the main functions of mitochondria is the generation of ATP through the respiratory chain. In *Plasmodium* blood stages, however, the energy metabolism relies largely on glycolysis (29, 30), and the gain of ATP through the mtETC is considered only marginal (31). It has been suggested that the main function of the mtETC might be to provide the electron acceptor CoQ (ubiquinone) for DHOD, a key enzyme for the essential *de novo* biosynthesis of pyrimidine (4). The $\Delta\psi_m$, in turn, is essential for

* This work was supported by the Max Planck Society and partly by grants from the EviMalar network of excellence (#34).

[S] The on-line version of this article (available at http://www.jbc.org) contains supplemental Movies 1 and 2, Figs. 1–6, and Table 1.

[1] To whom correspondence should be addressed: Parasitology Unit, Max Planck Institute for Infection Biology, Charitéplatz 1, 10117 Berlin, Germany. Tel.: 49-30-28460535; Fax: 49-30-28460225; E-mail: matuschewski@mpiib-berlin.mpg.de.

[2] The abbreviations used are: mtETC, mitochondrial electron transport chain; DHOD, dihydroorotate dehydrogenase; HDQ, dodecylquinolin-4-ol,1-oxide; NDH2, NADH:ubiquinone dehydrogenase; Q, ubiquinone (coenzyme Q); QH_2, ubiquinol; *Pb*-, *P. berghei*.

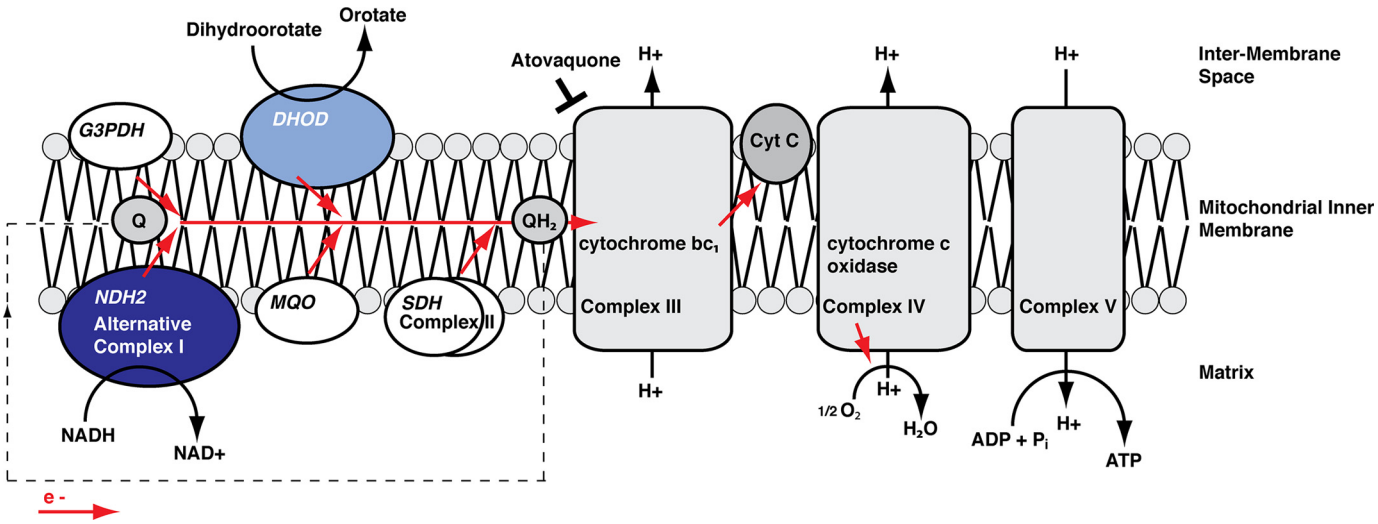

FIGURE 1. **Hypothetical model of the mitochondrial NADH:oxidoreductase NDH2 in the mtETC of the malarial parasite.** Shown is a schematic of the localization and biochemical function of *Pb*NDH2 (*dark blue ellipse*). The precise localization to either the internal (mitochondrial matrix) or the external (inter-membrane space) side of the mitochondrial inner membrane remains to be determined. Together with four other *Plasmodium* mitochondrial dehydrogenases (DHOD) malate:quinone oxidoreductase (*MQO*), glycerol-3-phosphate dehydrogenase (*G3PDH*), and succinate dehydrogenase (*SDH*)), NDH2 likely acts as an electron donor in the mtETC, reducing ubiquinone (*Q*) to ubiquinol (QH_2). DHOD (*light blue ellipse*), as part of the pyrimidine biosynthesis pathway, is thought to be essential. The antimalarial drug atovaquone targets the complex III, thereby inhibiting the reoxidation of QH_2 to Q.

transport processes, for example in the heme biogenesis pathway (32). However, $\Delta\psi_m$ does not rely exclusively on the mtETC (4). Atovaquone, a Q analog, binds to cytochrome bc_I, thereby inhibiting the reoxidization of QH_2 to coenzyme Q and interrupting the mtETC. Atovaquone alone, however, does not lead to the collapse of the mitochondrial membrane potential. Furthermore, it has recently been shown that short time treatment with atovaquone and proguanil exerts a stage-specific and cytostatic effect on *P. falciparum* blood stages *in vitro* (33) with ring- and schizont stages being able to survive the interruption of the mtETC as well as the collapse of the $\Delta\psi_m$ for as long as 48–96 h, whereas trophozoites proved to be more sensitive.

In this study we addressed the *in vivo* role of *NDH2* in the rodent malaria model parasite *Plasmodium berghei*. We could identify an essential function for parasite growth and, as a consequence, sporozoite formation inside the mosquito vector. Our data suggest that the *Plasmodium* alternative type I complex is dispensable for life cycle progression in the vertebrate host.

EXPERIMENTAL PROCEDURES

Experimental Animals—All animal work was conducted in accordance with the German "Tierschutzgesetz in der Fassung vom 18. Mai 2006 (BGBl. I S. 1207)" which implements the directive 86/609/EEC from the European Union and the European Convention for the protection of vertebrate animals used for experimental and other scientific purposes. The protocol was approved by the ethics committee of MPI-IB and the Berlin state authorities (LAGeSo Reg# G0469/09). Animals were from Charles River Laboratories.

Gene Expression Profiling—For quantitative real-time-PCR analyses, poly(A)+ RNA was isolated using oligo-dT columns (Invitrogen) from mixed blood stages, ookinetes, oocysts, salivary gland-associated sporozoites, and 24-h liver stages of *P. berghei* wild-type (WT) parasites. After DNase treatment, the mRNA of each sample was reverse-transcribed to cDNA using oligo-dT primers (Ambion). Specificity of the amplification products was confirmed by melting curve analysis; a no-template control was added in every run. For primers, see supplemental Table 1. In our experiments, each RT-PCR run was carried out in triplets of one mRNA pool, and the whole series was reproduced in a second independent experiment.

Gene Targeting Vectors and P. berghei Transfection—For mCherry tagging of *PbNDH2*, we cloned a C-terminal fragment of 1194 bp into a standard transfection vector, which contained the mCherry coding sequence using primers NDH2-mCherry_for and NDH2_mCherry_rev. After linearization of the plasmid, transfection, and a single crossover event, we obtained parasites with the tagged full-length NDH2. Genotyping was performed using primers 5′integration_for and 5′KO_flank_rev and WT_for and WT_rev for transgenic and WT parasites, respectively. For gene deletion of *PbNDH2*, a replacement vector was generated by cloning two fragments, 5′ KO flank (649 bp) and 3′ KO flank (651 bp), into the standard transfection vector (34) using *P. berghei* genomic DNA as a template and the following primer combinations (see supplemental Table 1): 5′_KO_flank_for and 5′_KO_flank_rev, and 3′_KO_flank_for and 3′_KO_flank_rev. For replacement-specific amplification of the *ndh2*(−) locus, the following primer pairs were utilized: in the 5′ region, 5′_integration_for and 5′_integration_rev; the 3′ region, 3′_integration_for and 3′_integration_rev. To validate the purity of the clonal *ndh2*(−) population, an *NDH2*-specific amplification using WT_for and WT_rev was performed. Two independent *ndh2*(−) parasite populations, termed ko1 and ko2, from two consecutive transfections and subsequent *in vivo* clonings were obtained. After verification of the phenotypical identity, one representative clone of each ko1 and ko2 was used for a detailed analysis. The Southern blot was done using the PCR DIG probe synthesis kit and the DIG Luminescent Detection kit (Roche Applied Science) according to the manufacturer's instructions.

Plasmodium Life Cycle and Phenotypic Analysis of Mutant Parasites—Anopheles stephensi mosquitoes were kept at 21 °C, 80% humidity, and daily feeding on 10% sucrose. Asynchronous blood stages of *P. berghei* ANKA-GFP (WT) (34) and *ndh2*(−) parasites were maintained in NMRI mice and checked for gametocyte formation and exflagellation of microgametes before mosquito feeding. Exflagellation events were found to be similar, with ~3900/μl (WT), ~7200/μl (*ndh2*(−) ko1), and ~2700/μl (*ndh2*(−) ko2) observed within a period from ~10 to 16 min after taking blood from the infected mouse. For the subsequent mosquito infection, age-matched *A. stephensi* mosquitoes were allowed to blood-feed on the anesthetized mice for 15 min. For mosquito infection with cultured ookinetes, age-matched mosquitoes were membrane fed with 3,500,000 ookinetes of each WT, *ndh2*(−) ko1, and *ndh2*(−) ko2. Dissection of mosquitoes was conducted at days 10, 14, 17, and 21 to determine infectivity and sporozoite numbers in midguts and salivary glands, respectively. For transmission electron microscopy, infected midguts were fixed in 2.5% glutaraldehyde. To obtain exo-erythrocytic forms, the hepatocytes of the cell line HuH7 were infected with salivary gland sporozoites and cultured for 24–48 h.

Immunofluorescence and Mitochondrial Staining—Parasites were fixed with 4% paraformaldehyde and permeabilized with 1% Triton X-100. Immunofluorescence was done with previously described monoclonal antibodies against *P. berghei* circumsporozoite protein (35) and Hsp70 (36). Oocysts were stained with either antibodies against circumsporozoite protein or GFP (Abcam), and the *NDH2-mCherry* signal was enhanced using anti-mCherry antibodies (Chromotek). Mitochondria were stained with MitoTracker Green FM (Invitrogen) according to the manufacturer's instructions. MitoTracker Green FM is not retained well after fixation, but in our hands at a concentration of 500 nM, subsequent fixation of parasites with 4% paraformaldehyde and permeabilization with methanol led to satisfying results. To detect the mitochondrial membrane potential, JC-1 (Sigma) was used on WT and *ndh2*(−) ookinetes according to the manufacturer's instructions. Ookinetes were incubated in JC-1 staining solution for 20 min at 20 °C and observed under the fluorescent microscope within 20 min.

Purification of Ookinetes and Recording Ookinete Motility—Ookinetes were cultured (37) and purified with p28-labeled magnetic beads (Dynabeads, Sigma) as described (38). Ookinetes gliding in Matrigel were filmed for 10 min and then tracked using ImageJ.

RESULTS

NDH2 Is Expressed in Multiple Plasmodium Life Cycle Stages and Localizes to Mitochondria—We initiated our analysis by profiling the expression of *NDH2* transcripts in different extra- and intracellular stages of the *P. berghei* life cycle (Fig. 2*A*). Using cDNA as template we could readily identify *NDH2* mRNA in mixed blood stages, purified ookinetes, midgut-associated oocysts, and liver stage trophozoites (24 h after infection). Although transcript levels varied slightly in these stages, the most prominent exception of *NDH2* expression was purified salivary gland-associated sporozoites, which had a significantly reduced (>300-fold) level as compared with all other stages tested.

We next generated a parasite line, termed *NDH2mCherry*, which was obtained by insertional tagging of the endogenous *NDH2* open reading frame by in-frame fusion of mCherry at the C terminus (Fig. 2*B*). For this purpose we designed a targeting vector that contained a 5′ deleted copy of *NDH2* fused to the mCherry protein (39). Upon single crossover by restriction endonuclease-mediated homologous recombination and positive selection with the antifolate pyrimethamine, this vector is predicted to result in a functional, mCherry-tagged 5′ and a non-functional, promoter-less and N-terminal-deleted 3′ copy, separated by the positive selection marker (Fig. 2*B*). Genotyping of the pyrimethamine-resistant parasite line after *in vivo* cloning by limited dilution revealed the desired parasite clone, which no longer contained wild-type parasites (Fig. 2*C*).

We used the *NDH2mCherry* parasites to monitor expression in the mammalian and insect hosts. Live cell imaging based on mCherry signals revealed only faint signals.[3] We, therefore, fixed and stained parasites with an anti-mCherry antibody (Fig. 2*D*). This approach revealed a number of important findings with respect to the expression and localization of NDH2. Unexpectedly, no robust mCherry signal was detected in asexual blood stages, as exemplified in intracellular trophozoites. In contrast, gametocytes, the sexual forms of the blood stage development, consistently displayed an intense punctuate or branched[3] staining, indicative of abundant NDH2 protein that localizes to a cellular organelle, most likely the *Plasmodium* mitochondrion. NDH2 expression in gametocytes also explains the expression obtained by mRNA profiling in mixed blood stages (Fig. 2*A*). Expression continued in ookinetes, in good agreement with the transcript analysis. In ookinetes, a prominent concentration of the signal in a branched structure adjacent to the parasite nucleus was detectable. NDH2 protein was prominent in oocysts and late liver stages but absent in sporozoites, further corroborating the transcript profiles (Fig. 2*A*). Together, we conclude that NDH2 is most prominently expressed in gametocytes, ookinetes, oocysts, and liver stages and virtually absent in asexual blood stages and sporozoites.

The immunofluorescence analysis of the *NDH2-mCherry* parasites was already suggestive of the expected localization of NDH2 to the parasite mitochondria. To unequivocally show mitochondrial localization, we used MitoTracker, an organelle-specific fluorescent dye (Fig. 2*E*). We analyzed gametocytes and ookinetes, where NDH2 expression is robust. The mCherry signal showed perfect overlap with the MitoTracker, corroborating proper localization of NDH2 to the mitochondria.

Ablation of NDH2 Does Not Affect Growth of Asexual Blood Stage Parasites—We next wanted to test *in vivo* essentiality of *NDH2* by targeted gene deletion. For this purpose, we employed experimental genetics and targeted the gene by double cross-over recombination (Fig. 3*A*). As predicted from the expression analysis (Fig. 2*D*) but in stark contrast with the proposed candidacy as an anti-malaria drug target (15, 24, 40, 41), we were able to recover recombinant parasites that contained

[3] K. E. Boysen and K. Matuschewski, unpublished data.

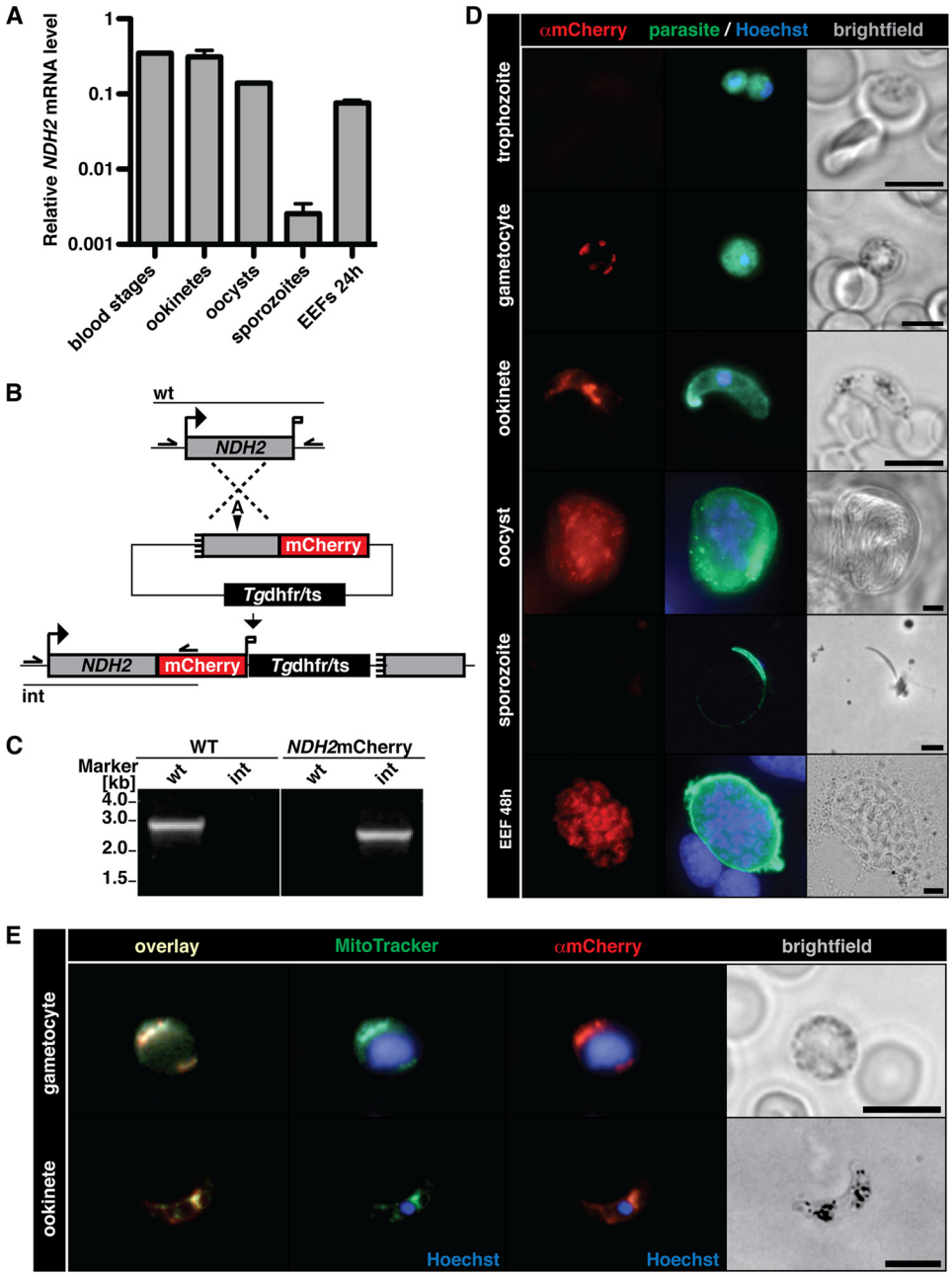

FIGURE 2. **The type II NDH2 is a mitochondrial protein in the malaria parasite.** *A*, expression profiling of *NDH2* by quantitative real time PCR is shown. Data were normalized to *GFP*, which is constitutively expressed under the *EF1α* promoter. Note the abundant *NDH2* transcripts in mixed blood stages and ookinetes and a prominent drop in mRNA levels in sporozoites. *B*, shown is the generation of *NDH2-mCherry* parasites. The *NDH2* genomic locus was targeted with a replacement plasmid containing the C-terminal *NDH2* fragment (*gray box*) fused in-frame to the *mCherry* coding sequence (*red*). In addition, the targeting plasmid contains the *Tgdhfr/ts*-positive selectable marker (*black box*). Upon a single crossover event, the targeting plasmid is expected to generate an mCherry-tagged *NDH2* ORF and a non-expressed truncated fragment, shortened by 446 bp. *Arrows* and *bars* indicate specific primers and PCR fragments, respectively. *A*, AflII. *C*, genotyping of *NDH2-mCherry* parasites is shown. Integration of the mCherry tag (*int*) and absence of WT parasites (*wt*) confirmed the presence of a clonal *NDH2-mCherry* parasite population. *D*, epifluorescence images of *NDH2-mCherry* parasites during the entire life cycle are shown. Intra- or extracellular parasites were fixed, permeabilized, and stained with anti-mCherry (*red*) or anti-parasite (*green*) antibodies, and nuclei were visualized with Hoechst stain (*blue*). *Bars*, 5 μm. Note the absence of a mCherry signal in trophozoites and sporozoites. *EEF*, exo-erythrocytic form. *E*, *NDH2* localizes to the mitochondrion of the parasite. Gametocytes and ookinetes of the *NDH2-mCherry* clone were incubated with MitoTracker Green FM (*green*), then fixed, permeabilized, and stained with anti-mCherry antibodies (*red*). *Bars*, 5 μm.

the deletion of *NDH2*, as confirmed by PCR-based genotyping (Fig. 3*B*) and quantitative RT-PCR (Fig. 3*C*). This finding already indicated that loss of *NDH2* function is compatible with parasite survival inside host erythrocytes *in vivo*.

To test whether other mitochondrial NADH-dependent dehydrogenases are up-regulated in *ndh2*(−) parasites and can potentially compensate for loss of *NDH2* function, we performed quantitative PCR in WT and *ndh2*(−) mixed blood stages for glycerol-3-phosphate dehydrogenase (*G3PDH*), DHOD, malate:quinone oxidoreductase (*MQO*), and succinate dehydrogenase (*SDH*) (Fig. 3*D*). This analysis confirmed complete absence of *NDH2* transcripts in the knock-out parasite line and showed no compensatory up-regulation of any of the dehydrogenases tested.

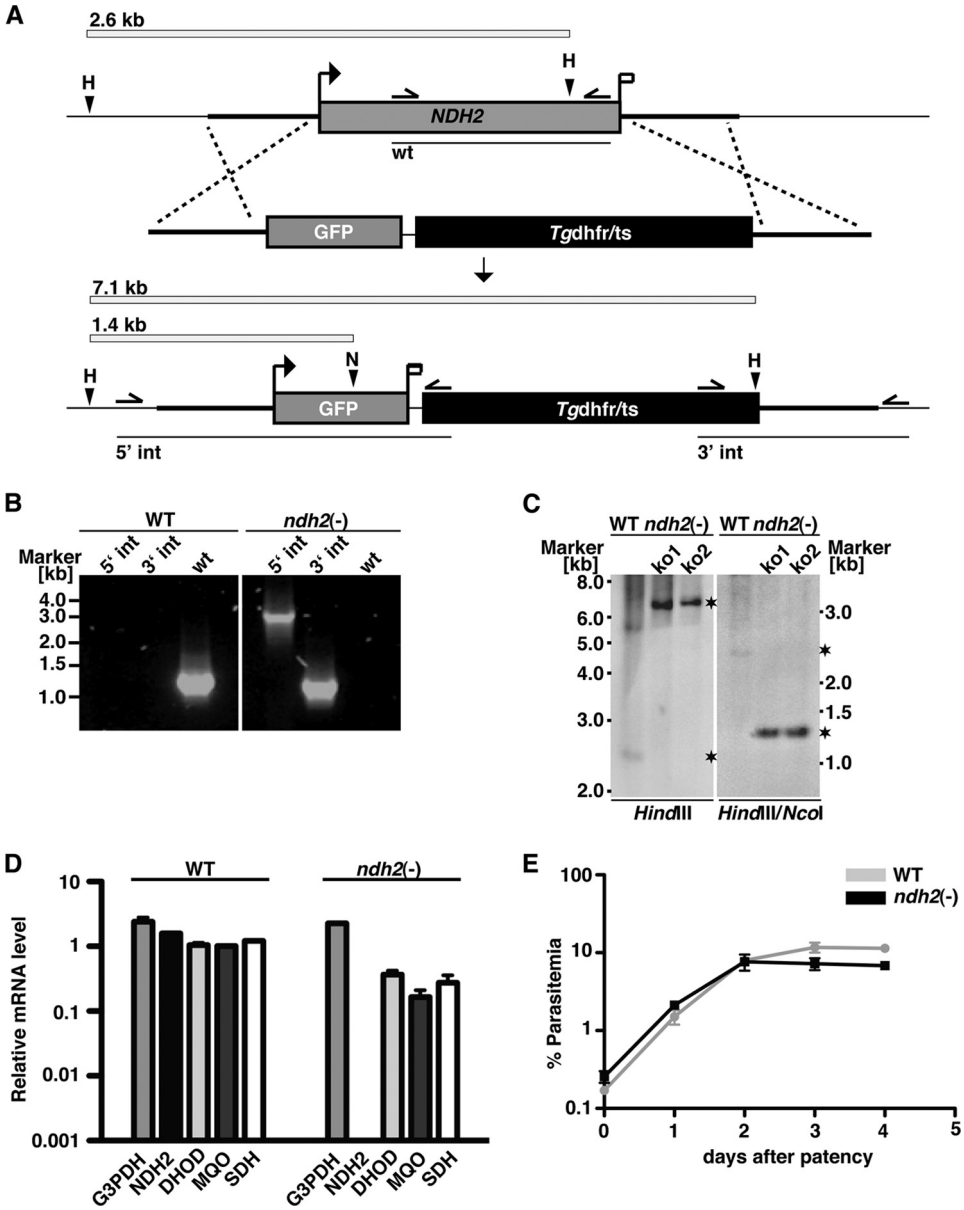

FIGURE 3. ***P. berghei NDH2* is dispensable for asexual blood stages.** *A*, the wild-type *NDH2* locus is targeted with a linearized replacement plasmid containing the 5′- and 3′-UTRs of *PbNDH2*, *GFP*, and the positive selection marker *Tgdhfr/ts*. After double crossover homologous recombination, the *NDH2* open reading frame is substituted by *GFP* and the selection marker, resulting in the loss-of-function *ndh2*(−) allele. GFP is now expressed under the *PbNDH2* promoter and, therefore, indicates *PbNDH2* promoter activity. Replacement- and WT-specific test primer combinations, expected PCR fragments, and predicted sizes of restriction endonuclease fragments are shown as *arrows*, *lines*, and *white bars*, respectively. *H*, HindIII; *N*, NcoI. *B*, confirmation of the *NDH2* gene disruption by replacement-specific PCR analysis with primer combinations that amplify a signal in the recombinant locus (*5′ int* and *3′ int*) only. The absence of a WT-specific signal in the clonal *ndh2*(−) population confirms the purity of the mutant parasite line. *C*, a Southern blot confirms the desired *NDH2* deletion in two clones from two independent transfections (*ko1* and *ko2*). Fragments are marked with *asterisks*. Restriction sites used for the digest of genomic DNA are indicated at the *bottom*. The 5′ flank of the targeting vector was used as probe for the Southern blot. *D*, quantitative RT-PCR from WT and *ndh2*(−) mixed blood stages is shown. Shown are transcript levels for glycerol-3-phosphate dehydrogenase (*G3PDH*; gi:68071805), *NDH2*, dihydroxyorotate dehydrogenase (DHOD; gi:68074653), malate:quinone oxidoreductase (*MQO*; gi:68075787), and succinate dehydrogenase (*SDH*; gi:68063151). Data were normalized to the putative aspartyl-tRNA synthetase (PBANKA_021020). Note the depletion of *NDH2* transcripts in *ndh2*(−) parasites. *E*, *ndh2*(−) parasites cause high level parasitemia *in vivo*. Displayed are *in vivo* growth curves of WT (*gray*) and knock-out parasites (*black*). Animals ($n = 3$) were injected intravenously with 1,000,000 asexual parasites of the respective parasite populations. Parasitemia was determined every 24 h after infection by microscopic examination of Giemsa-stained blood smears.

To corroborate our findings and detect potential minor growth defects, we next infected C57bl/6 mice by intravenous inoculation of 1,000,000 asexual blood stages of either WT or *ndh2*(−) parasites (Fig. 3*E*). *NDH2* loss-of-function parasites replicated with identical kinetics as compared with WT parasites, suggesting that ablation of *NDH2* is tolerated by *Plasmodium* parasites during the intra-erythrocytic replication cycle. Moreover, all animals ultimately displayed symptoms of cerebral malaria (supplemental Fig. 2), suggesting that *ndh2*(−) parasites retained virulence and the capacity to induce experimental cerebral malaria *in vivo*. We conclude that targeted design of potential specific NDH2 inhibitors would not aid in development of new anti-malarial drugs.

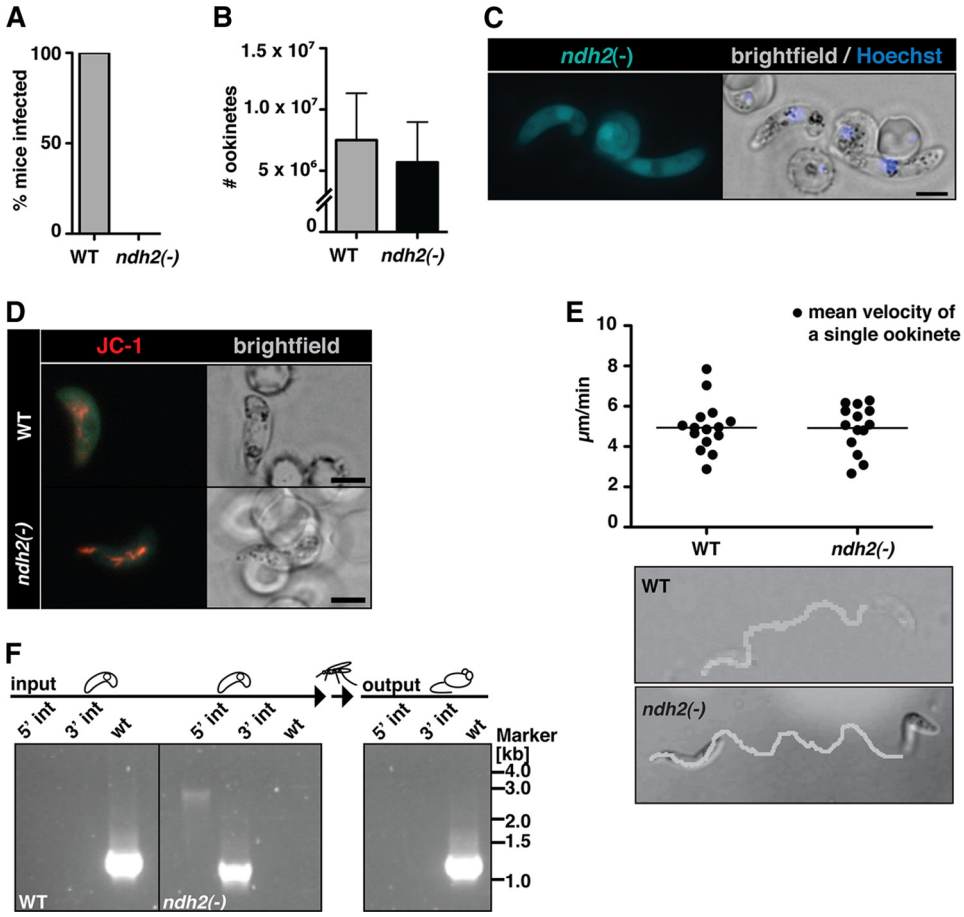

FIGURE 4. **Ablation of *NDH2* does not affect host switch from mammals to the insect vector.** *A*, shown is a *Plasmodium* transmission experiment. Naïve mice were exposed to WT- or *ndh2*(−)-infected *A. stephensi* mosquitoes and examined daily for a blood stage infection. Data are from 3 separate experiments, with 2 *ndh2*(−) clones generated through separate transfection experiments and a total of 10 recipient mice. *B*, ookinete formation is not affected by the absence of *NDH2*. Ookinetes were formed *in vitro* in culture medium and quantified. Data are based on four *in vitro* cultures for each WT and *ndh2*(−). *C*, shown is epifluorescence live microscopy of a *ndh2*(−) ookinete. GFP expression confirms activity of the *NDH2* promoter during sexual differentiation, ookinete viability, and successful integration of GFP into the *NDH2* locus. *Bar*, 5 μm. *D*, mitochondrial membrane potential is detectable in WT and *ndh2*(−) ookinetes. Ookinetes were stained with the live stain JC-1, which forms red fluorescent aggregates in mitochondria if the membrane potential is intact. *Bar*, 5 μm. *E*, ookinete velocity is not affected by ablation of *NDH2*. Ookinetes in Matrigel were filmed for ~10 min, and their tracks were quantified. Representative images of an *ndh2*(−) and a WT ookinete track (*bottom*) and mean velocity of WT ookinetes ($n = 15$) and *ndh2*(−) ookinetes ($n = 14$) (*top*) are shown. Note that all *ndh2*(−) ookinetes displayed gliding locomotion ($n = 43$).[3] *F*, inability of *ndh2*(−) parasites to complete the life cycle is shown. A mix of both WT and KO ookinetes was membrane-fed to mosquitoes. After bite back, only WT blood stages could be detected in mice. Integration of KO construct and the absence of WT was monitored with PCR on genomic DNA derived from blood stage infection before setting up and mixing ookinete cultures (*input*) and after bite back (*output*).

NDH2 Is Dispensable for Mouse-to-Mosquito Host Switch— To explore whether *NDH2* plays any important role during *Plasmodium* life cycle progression, we first infected *A. stephensi* with WT and *ndh2*(−) parasites and tested whether these infected mosquitoes can, 3 weeks later, induce a malaria infection in naïve mice (Fig. 4*A*). In three independent transmission experiments, none of the recipient mice developed a patent malaria infection, indicative of a major role at some point during the *Plasmodium* life cycle.

The apparent vital role of *NDH2* prompted us to study life cycle progression of *ndh2*(−) parasites in infected *Anopheles* mosquitoes. We first examined the viability of sexual stages, termed gametocytes, and transmission stages, termed ookinetes. Because gametocytes were present in similar proportions as in WT parasites and exflagellation was indistinguishable from WT-infected blood,[3] we cultured ookinetes *in vitro* from infected animals. Total ookinete numbers were similar in WT and *ndh2*(−) cultures, indicating a successful developmental switch in the absence of a functional NDH2 enzyme (Fig. 4*B*).

To substantiate viability of *ndh2*(−) ookinetes, we took advantage of the GFP expression under the endogenous *NDH2* promoter generated through our gene replacement strategy (Fig. 3*A*). We observed brightly fluorescent, viable gametocytes and ookinetes (Fig. 4*C*). This finding also served as an independent confirmation for the expression profiling of *NDH2* (Fig. 2, *A* and *D*). The notion that *ndh2*(−) retained their full viability was further supported by the detection of the mitochondrial membrane potential through incubation with the fluorescent dye JC-1 (42, 43) in WT and mutant parasites (Fig. 4*D*). We next documented and quantified cellular motility, termed gliding locomotion, of cultured *ndh2*(−) and WT ookinetes (Fig. 4*E*, supplemental Movies 1 and 2). In Matrigel, *ndh2*(−) ookinetes performed the signature corkscrew movements at a pace that is indistinguishable from WT ookinetes.

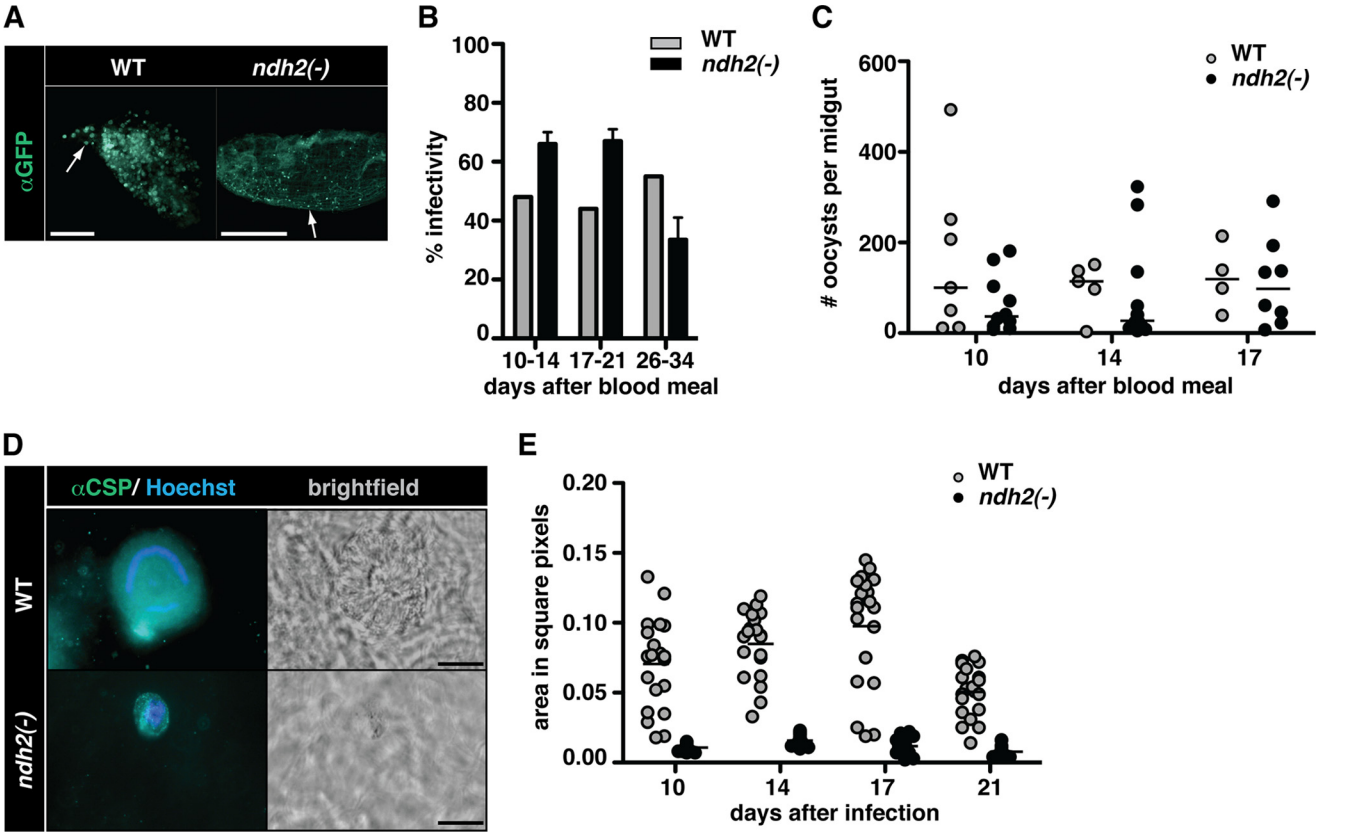

FIGURE 5. ***ndh2*(−) parasites are arrested in oocyst maturation.** *A*, shown is successful colonization of midguts after transmission to *A. stephensi*. Mosquitoes were allowed to feed on WT- and *ndh2*(−)-infected mice, and midguts were removed 17 days later. Oocysts are visualized with an anti-GFP antibody. Note that *ndh2*(−) oocysts are much smaller. *Arrows* point at single oocysts. *Bar*, 500 μm. *B*, infectivity of WT- and *ndh2*(−)-infected *A. stephensi* midguts were isolated on the days indicated after a blood meal on infected mice and submitted to immunofluorescence analysis. The infectivity was similar in WT- and *ndh2*(−)-infected mosquitoes. Experiments were performed with two *ndh2*(−) clones generated through separate transfection experiments. *C*, oocyst numbers are similar in WT- and *ndh2*(−)-infected mosquitoes. Oocysts were scored from infected midguts between days 10 and 17 after the blood meal. The median is shown. The Mann-Whitney test was applied for every day indicated and revealed no significant differences in oocyst numbers. *D*, arrested oocyst growth of *ndh2*(−) parasites. Shown are representative oocysts from WT- and *ndh2*(−)-infected mosquitoes. Oocysts were stained with an anti-circumsporozoite protein (*αCSP*) antibody 16 days after infection. Note that *ndh2*(−) oocysts are clearly visible but significantly smaller than WT oocysts. WT oocysts show the typical circular stain of nuclei in sporoblasts. In *ndh2*(−) oocysts DNA can be stained but appears unorganized. *Bar*, 20 μm. *E*, shown is a quantification of oocyst size. Oocyst sizes in square pixels were measured using ImageJ. WT, $n = 40$; *ndh2*(−), $n = 40$.

To support our earlier finding of an important role in life cycle progression and to exclude any mosquito-related inhibition of transmission, we membrane-fed a mix of separately cultured WT and *ndh2*(−) ookinetes to mosquitoes (Fig. 4*F*). After maturation in the insect vector and transmission to naïve mice, only WT parasites were recovered. We conclude that presence of *NDH2* is not important for viability and cellular migration of ookinetes, the mammal-to-mosquito transmission stages, but at some point after host switch from the mouse to the mosquito vector.

Arrested Oocyst Maturation in ndh2(−) Parasites—We next examined oocyst development that occurs at the outer side of the mosquito midgut (Fig. 5). When we isolated midguts from *A. stephensi* mosquitoes that had fed on WT- or *ndh2*(−)-infected mice 10 days earlier, we noticed abundant oocysts that were reactive with anti-circumsporozoite protein antibodies (Fig. 5*A*). Infectivity, *i.e.* the proportion of oocyst-positive insects, was similar in WT- and *ndh2*(−)-infected mosquitoes irrespective of natural transmission or membrane feedings with cultured ookinetes and remained constant over time (Fig. 5*B*). When we scored the total numbers of oocysts, again no differences were detected between mosquitoes infected with the two parasite populations (Fig. 5*C* and supplemental Fig. 3). As predicted, the number of oocysts in mosquitoes after membrane feeding was lower for both WT and *ndh2*(−) parasites compared with after natural feeding (supplemental Fig. 3). We conclude that *ndh2*(−) parasites establish infections in the insect vector similar to WT parasites.

Upon closer inspection we noticed that *ndh2*(−) oocysts were considerably smaller than oocysts from WT-infected mosquitoes (Fig. 5*D*). Quantification of oocyst sizes revealed largely reduced *ndh2*(−) oocysts (Fig. 5*E*). Prolonged development did not improve sporogony, resulting in the complete failure to produce sporozoites (supplemental Fig. 4). We conclude that *NDH2* is vital for sporogony. In the absence of this mitochondrial protein, life cycle progression is completely blocked inside the insect vector.

Developmental Defects in Oocysts Lacking NDH2—To gain further insight into oocyst development of *ndh2*(−) parasites, we employed transmission electron microscopy (Fig. 6). We observed fully rounded oocysts with apparently intact oocyst walls, indicating that initial transition from ookinete to oocyst is not impaired by the absence of *NDH2*. We could also consistently identify mitochondria with the typical tubular cristae

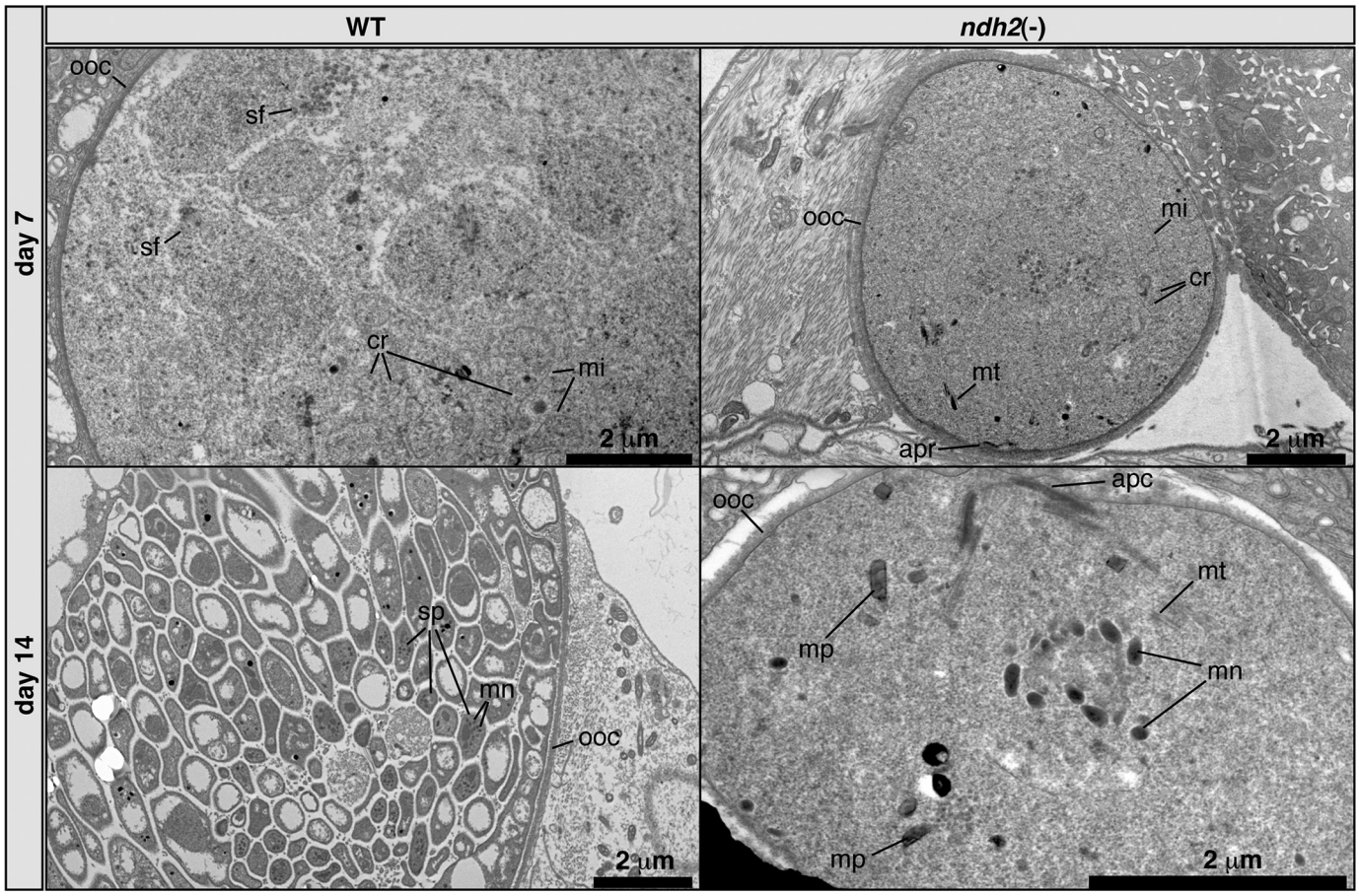

FIGURE 6. **Morphology of *ndh2*(−) and WT oocysts.** Transmission electron microscopy shows low levels of organization in *ndh2*(−) oocysts and no sign of sporogony. Cristate mitochondria can be detected in both WT and KO oocysts. Note that *ndh2*(−) oocysts contain remnants of ookinete organelles, including the apical complex (*lower right panel*). Structures such as cristae and malaria pigment were identified by comparison with published electron microscope pictures (65, 66). *apc*, apical complex; *apr*, apical polar ring; *cr*, cristae; *mi*, mitochondrion; *mn*, micronemes; *mp*, malaria pigment; *mt*, microtubules; *ooc*, oocyst wall; *sf*, spindle fibers. *sp*, sporozoite.

(Fig. 6 and supplemental Fig. 6). However, the overall level of organization in mutant oocysts was low compared with WT oocysts. We could not detect any sporozoite formation. Strikingly, we repeatedly detected remnants of ookinete-related structures in *ndh2*(−) oocysts (Fig. 6), such as the apical complex, microtubules, and micronemes. This finding is unprecedented and bears resemblance to an ookinete surrounded by oocyst cytoplasm. We detected these structures up until day 14 after infection, indicative of a defect in proper ookinete disintegration. We conclude that *NDH2* is vital for multiple developmental processes during oocyst maturation in the mosquito vector.

ndh2(−) Parasites Are Infectious to the Mammalian Host When Complemented during Sporogony—We finally wanted to test whether *ndh2*(−) parasites display an additional defect after transmission to the mammalian host, *i.e.* during preerythrocytic mammalian stages. Ookinetes and sporozoites are tetraploid and haploid, respectively. Previous work established that heterozygous oocysts, obtained by crossing mutant and WT parasites *in vivo*, can rescue loss-of-function mutants if defects are restricted to sporogony (44, 45). For the present study we crossed *ndh2*(−) and WT blood stage parasites (*input*) and genotyped the mixed parasites in comparison with clonal parasites before and after mosquito transmission (Fig. 7). After bite back of mosquitoes infected with the mixed population, the *ndh2*(−) genotype was recovered from blood stage infection in mice (*output*), strongly suggesting that the essential *in vivo* function of *Plasmodium NDH2* is restricted to the insect vector stages.

DISCUSSION

Our data show that *NDH2* plays a vital role for sporogony inside the invertebrate definitive host but not during asexual blood stage development in the warm-blooded intermediate host. *Plasmodium* parasites encounter considerable environmental changes upon transmission from the vertebrate to the insect vector, reflected by fundamental changes in morphology and gene expression of the parasite (46, 47). The sexual phase of *Plasmodium* ends with fertilization of the macrogamete in the midgut lumen and subsequent development into a motile zygote, the so-called ookinete. The ookinete then traverses the midgut wall and settles between the midgut epithelium and the basal lamina, where it develops into the sessile oocyst. Parasites are now extracellular, in contrast to replicative stages inside the mammalian host. They are exposed to ambient temperatures, more oxygen, and of particular importance in view of their energy metabolism, to a glucose-deprived environment.

NDH2 Is Most Abundant in Cristate Mitochondria—Data based on microarray and proteomic studies have shown before

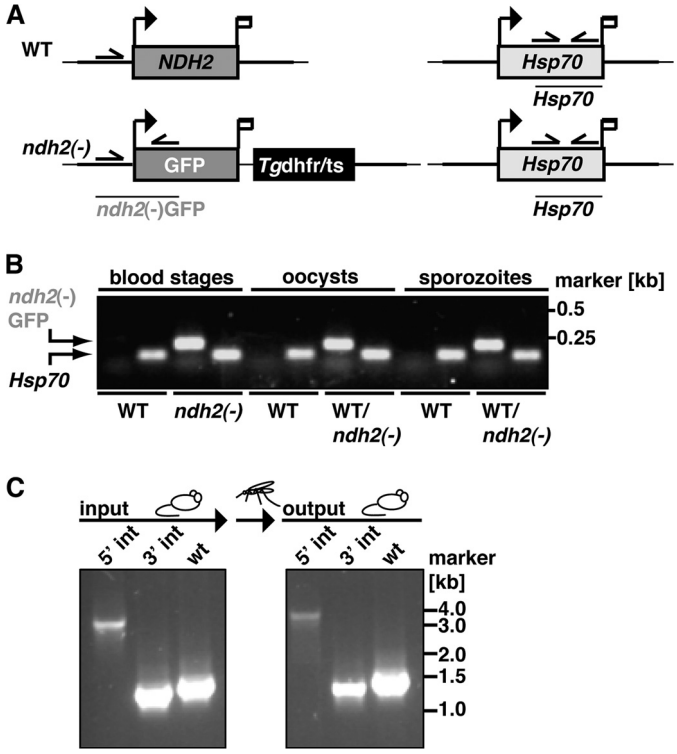

FIGURE 7. **NDH2 is essential for oocyst maturation only.** *A*, shown is a schematic of WT (*top*) and *ndh2*(−) (*bottom*) cDNA isolated after the complementation experiment. Primers are indicated with *arrows*. Diagnostic fragments, *i.e. ndh2*(−) GFP for *ndh2*(−) parasites and *Hsp70* as a positive control, are shown as *lines*. *B*, shown is the presence of *ndh2*(−) parasites in oocyst- and salivary gland-derived sporozoites after a blood meal on a mouse infected with a mixture of WT and *ndh2*(−) parasites (*input* in C). Real time-PCR products were analyzed by gel electrophoresis. *ndh2*(−)GFP was amplified in all mixed samples (WT/*ndh2*(−)) but not in WT. *C*, *ndh2*(−) sporozoites establish a blood stage infection. After bite back and isolation of *Plasmodium* genomic DNA, *ndh2*(−) blood stage parasites could be detected (*output*) by diagnostic PCR. Primers correspond to those shown in Fig. 3*A*.

that some members of the mitochondrial electron transport chain are up-regulated in oocysts compared with asexual blood stages, such as the FAD-dependent glycerol-3-phosphate dehydrogenase and cytochrome *c* (48, 49). We found that *NDH2* transcripts can be detected in most phases of the parasite life-cycle, and using an endogenous tagging approach, we show that NDH2 is most abundant in gametocytes, ookinetes, oocysts, and liver stages. The notion that the NDH2-mCherry fusion protein is functional is supported by localization to parasite mitochondria and functional complementation of the developmental arrest of *NDH2* loss of function parasites.

Remarkably, abundance of NDH2 correlates with the cristate stage of the mitochondrion. For *P. berghei*, cristae have been reported for pre-erythrocytic stages (50), gametocytes, sporogonic stages (51), and oocysts (52, 53), whereas trophozoites were termed acristate (51). Similarly, few cristae were found in asexual stages of *P. falciparum* and more in gametocytes (54, 55). Apparently, *Plasmodium* mitochondria undergo distinct switches from cristate (sexual and mosquito stages) to acristate stages (asexual erythrocytic stages) and back (55). Cristae are invaginations of the inner membrane, providing a greater surface for the complexes of the mtETC, thus allowing for a higher rate of ATP metabolism. For instance, it has been shown that the activity of succinate dehydrogenase is high in cristate but low in acristate mitochondria (56). Therefore, abundant expression of NDH2mCherry might reflect the increase in surface of the mitochondrial inner membrane, which in turn would lead to a higher capacity to integrate NDH2. We found that mitochondria in *ndh2*(−) oocysts, the point of life cycle arrest, are clearly cristate, similar to those of WT oocysts.

NDH2 Is Vital Only for Oocyst Maturation—It has been proposed that the mtETC might be particularly important in non-erythrocytic stages (48, 57). We now provide genetic evidence to support this hypothesis. Our findings that ablation of *NDH2* is tolerated in disease-causing asexual blood stages but lethal during oocyst maturation and that transient trans-complementation during sporogony leads to successful life cycle progression suggests that NDH2 is needed, most likely as an electron donor, in oocysts. A plausible assumption is that NDH2 assures sufficient supply of ATP during sporogony in the insect vector. However, NDH2 does not seem to be essential for the branching or segregation of mitochondria. The latter has to take place not only during the sporozoite budding process in oocysts but also in liver and blood schizogony to assure that merozoites receive a single mitochondrion. None of these processes was affected by the deletion of *NDH2*, as we could show by complementing *ndh2*(−) with WT parasites; once *ndh2*(−) parasites had been rescued from arrest during oocyst maturation, they were able to complete the life cycle and establish blood stage infections.

In a preliminary experiment we used HDQ to test its effect on *P. berghei* WT and *ndh2*(−) blood stages *in vivo*. HDQ was thought to target *P. falciparum* NDH2 (16) but was more recently shown to likely inhibit DHOD (19, 25). We speculated that the absence of NDH2 in combination with HDQ treatment might show a stronger effect than HDQ treatment alone. However, at a concentration of 50 mg/kg bodyweight, HDQ had no effect on parasite growth *in vivo* (supplemental Fig. 4) either in WT or *ndh2*(−) parasites. Interestingly, 32 mg of HDQ/kg bodyweight has been shown to affect *Toxoplasma gondii* growth *in vivo* (58). We interpret these findings as an indication for potential differences in energy requirements and ATP generation between *Plasmodium* parasites and *T. gondii*.

NDH2 Is Not Vital for Maintenance of the Mitochondrial Membrane Potential—We show in ookinetes that the mitochondrial membrane potential was not abolished in the absence of *NDH2*. Although this finding casts doubt on the proposed role of NDH2 as one of the main suppliers of electrons to the mtETC (22), a possible explanation is that only a marginal electron flux is necessary to maintain the mitochondrial membrane potential because of the overall low level of ATP synthesis. Alternatively, reverse action of the F0F1 ATP synthase, *i.e.* ATP hydrolysis, might maintain the mitochondrial membrane potential for some time. Such a reverse role has for instance been demonstrated for *Trypanosoma brucei* and *Tetrahymena thermophila* (59, 60). Although reverse action of F0F1 ATPase has not yet been shown for *Plasmodium*, the components of the enzyme have been identified (61).

We were unable to employ JC-1 in *ndh2*(−) oocysts, mainly due to difficulties to unequivocally detect them among the metabolically active insect cells without fixation and immunofluorescence analysis.[3] We hypothesize that the membrane potential would be substantially impaired during sporogony, where

presumably more ATP needs to be generated through the mtETC, resulting in insufficient supply of electrons. However, we observed viable, *i.e.* GFP expressing, *ndh2*(−) oocysts for extended periods (day 21 after infection and beyond), which would suggest that the membrane potential is not completely abolished even in these stages.

Ablation of NDH2 Leads to Impairment of ATP-dependent Processes, Such as Organelle Disposal—The maturing oocyst needs ATP for a number of tasks, such as protein synthesis, mitosis, and processes involving actin polymerization. Within the first days of oocyst maturation, the parasite has to dispose of and possibly recycle ookinete-related organelles, such as micronemes and microtubules. The pathways of organelle clearance remain elusive. It was suggested that exocytosis, ubiquitylation, and autophagy all might play a role in the disposal of sporozoite organelles in early liver stages (62). Using electron microscopy, in *ndh2*(−) oocysts we have observed signature ookinete structures, such as the apical complex, micronemes, and microtubules, as late as 14 days after mosquito infection. We have also repeatedly observed spindle fibers on day 21, indicating viable oocysts but a delay in mitosis and/or the ATP-dependent process of chromosome segregation. We postulate that ablation of NDH2 results in delay and, ultimately, arrest of ATP-dependent processes needed for parasite remodeling during oocyst development.

Our findings raise the possibility that in the mammalian host ATP synthesis through the mtETC is dispensable for parasite development, whereas in the insect host this evolutionary conserved function is essential. Elegant genetic experiments established an essential role for the mtETC, via *DHOD*, for pyrimidine biosynthesis (4, 63, 64), during asexual blood stage development. However, this function was independent of ATP generation, which is mostly derived from glycolysis. NDH2 in turn, appears to be even dispensable as an electron donor for complex III to recycle ubiquinone for DHOD.

In conclusion, we provide experimental genetic evidence that *NDH2* is needed in a glucose-deprived environment, such as the mosquito. Candidacy of NDH2 as a promising drug target seems highly unlikely. However, at this stage we cannot formally exclude distinct roles, such as additional non-overlapping functions, of NDH2 paralogs in different *Plasmodium* species. Complementation of our *ndh2*(−) parasites with *P. falciparum NDH2* can only partially address this notion. In the absence of *in vivo* models for *P. falciparum,* essentiality of *P. falciparum NDH2* throughout the entire life cycle may be extrapolated from the findings described herein. In extension of our study, systematic analysis of the other mitochondrial dehydrogenases by experimental genetics in the rodent malaria model will inform design and preclinical research toward the identification of novel partner drugs for atovaquone.

Acknowledgments—We thank Dr. Wolfgang Bohne for HDQ, Professor Dr. Robert Sinden and Dr. Volker Brinkmann for critical comments on the electron microscope pictures, and Dr. Taco Kooij for providing plasmids. We are also indebted to Britta Laube for taking the electron microscope pictures and Volker Brinkmann for support in recording ookinete gliding motility.

REFERENCES

1. World Health Organization (2010) *World Malaria Report 2010*, World Health Organization Press, Geneva, Switzerland
2. World Health Organization (2010) *Global Report on Antimalarial Drug Efficacy and Drug Resistance: 2000–2010*, World Health Organization Press, Geneva, Switzerland
3. Petersen, I., Eastman, R., and Lanzer, M. (2011) *FEBS Lett.* **585,** 1551–1562
4. Painter, H. J., Morrisey, J. M., Mather, M. W., and Vaidya, A. B. (2007) *Nature* **446,** 88–91
5. Mather, M. W., and Vaidya, A. B. (2008) *J. Bioenerg. Biomembr.* **40,** 425–433
6. Vaidya, A. B. (1998) in *Malaria: Parasite Biology, Pathogenesis, and Protection* (Sherman, I. W., ed.) pp. 355–368, American Society for Microbiology, Washington, D. C.
7. Barton, V., Fisher, N., Biagini, G. A., Ward, S. A., and O'Neill, P. M. (2010) *Curr. Opin. Chem. Biol.* **14,** 440–446
8. Booker, M. L., Bastos, C. M., Kramer, M. L., Barker, R. H., Jr., Skerlj, R., Sidhu, A. B., Deng, X., Celatka, C., Cortese, J. F., Guerrero Bravo, J. E., Crespo Llado, K. N., Serrano, A. E., Angulo-Barturen, I., Jiménez-Díaz, M. B., Viera, S., Garuti, H., Wittlin, S., Papastogiannidis, P., Lin, J. W., Janse, C. J., Khan, S. M., Duraisingh, M., Coleman, B., Goldsmith, E. J., Phillips, M. A., Munoz, B., Wirth, D. F., Klinger, J. D., Wiegand, R., and Sybertz, E. (2010) *J. Biol. Chem.* **285,** 33054–33064
9. Malmquist, N. A., Gujjar, R., Rathod, P. K., and Phillips, M. A. (2008) *Biochemistry* **47,** 2466–2475
10. Phillips, M. A., and Rathod, P. K. (2010) *Infect. Disord. Drug Targets* **10,** 226–239
11. Davies, M., Heikkilä, T., McConkey, G. A., Fishwick, C. W., Parsons, M. R., and Johnson, A. P. (2009) *J. Med. Chem.* **52,** 2683–2693
12. Suraveratum, N., Krungkrai, S. R., Leangaramgul, P., Prapunwattana, P., and Krungkrai, J. (2000) *Mol. Biochem. Parasitol.* **105,** 215–222
13. Heymann, H., and Fieser, L. F. (1948) *J. Biol. Chem.* **176,** 1359–1362
14. Krungkrai, J., Kanchanarithisak, R., Krungkrai, S. R., and Rochanakij, S. (2002) *Exp. Parasitol.* **100,** 54–61
15. Biagini, G. A., Viriyavejakul, P., O'neill, P. M., Bray, P. G., and Ward, S. A. (2006) *Antimicrob. Agents Chemother.* **50,** 1841–1851
16. Saleh, A., Friesen, J., Baumeister, S., Gross, U., and Bohne, W. (2007) *Antimicrob. Agents Chemother.* **51,** 1217–1222
17. Mogi, T., Matsushita, K., Murase, Y., Kawahara, K., Miyoshi, H., Ui, H., Shiomi, K., Omura, S., and Kita, K. (2009) *FEMS Microbiol. Lett.* **291,** 157–161
18. Kawahara, K., Mogi, T., Tanaka, T. Q., Hata, M., Miyoshi, H., and Kita, K. (2009) *J. Biochem.* **145,** 229–237
19. Dong, C. K., Patel, V., Yang, J. C., Dvorin, J. D., Duraisingh, M. T., Clardy, J., and Wirth, D. F. (2009) *Bioorg. Med. Chem. Lett.* **19,** 972–975
20. Hatefi, Y., Haavik, A. G., and Griffiths, D. E. (1962) *J. Biol. Chem.* **237,** 1676–1680
21. Brandt, U. (2006) *Annu. Rev. Biochem.* **75,** 69–92
22. Fry, M., and Beesley, J. E. (1991) *Parasitology* **102,** 17–26
23. Melo, A. M., Bandeiras, T. M., and Teixeira, M. (2004) *Microbiol. Mol. Biol. Rev.* **68,** 603–616
24. Fisher, N., Bray, P. G., Ward, S. A., and Biagini, G. A. (2007) *Trends Parasitol.* **23,** 305–310
25. Rodrigues, T., Lopes, F., and Moreira, R. (2010) *Curr. Med. Chem.* **17,** 929–956
26. Patel, V., Booker, M., Kramer, M., Ross, L., Celatka, C. A., Kennedy, L. M., Dvorin, J. D., Duraisingh, M. T., Sliz, P., Wirth, D. F., and Clardy, J. (2008) *J. Biol. Chem.* **283,** 35078–35085
27. Kerscher, S. J. (2000) *Biochim. Biophys. Acta* **1459,** 274–283
28. Eschemann, A., Galkin, A., Oettmeier, W., Brandt, U., and Kerscher, S. (2005) *J. Biol. Chem.* **280,** 3138–3142
29. Hochachka, P. W., and Somero, G. N. (1984) *Biochemical Adaptation*, pp. 145–169, Princeton University Press, Princeton, NJ
30. Lang-Unnasch, N., and Murphy, A. D. (1998) *Annu. Rev. Microbiol.* **52,** 561–590
31. Olszewski, K. L., Mather, M. W., Morrisey, J. M., Garcia, B. A., Vaidya, A. B., Rabinowitz, J. D., and Llinás, M. (2010) *Nature* **466,** 774–778

32. Vaidya, A. B., and Mather, M. W. (2009) *Annu. Rev. Microbiol.* **63,** 249–267
33. Painter, H. J., Morrisey, J. M., and Vaidya, A. B. (2010) *Antimicrob. Agents Chemother.* **54,** 5281–5287
34. Janse, C. J., Franke-Fayard, B., Mair, G. R., Ramesar, J., Thiel, C., Engelmann, S., Matuschewski, K., van Gemert, G. J., Sauerwein, R. W., and Waters, A. P. (2006) *Mol. Biochem. Parasitol.* **145,** 60–70
35. Potocnjak, P., Yoshida, N., Nussenzweig, R. S., and Nussenzweig, V. (1980) *J. Exp. Med.* **151,** 1504–1513
36. Tsuji, M., Mattei, D., Nussenzweig, R. S., Eichinger, D., and Zavala, F. (1994) *Parasitol. Res.* **80,** 16–21
37. Sinden, R. E. (1997). in *The Molecular Biology of Insect Disease Vectors: A Methods Manual* (Crampton, J. M., Beard, C. B., and Louis, C., eds.) pp 67–91, Chapman & Hall, London
38. Sidén-Kiamos, I., Vlachou, D., Margos, G., Beetsma, A., Waters, A. P., Sinden, R. E., and Louis, C. (2000) *J. Cell Sci.* **113,** 3419–3426
39. Shaner, N. C., Campbell, R. E., Steinbach, P. A., Giepmans, B. N., Palmer, A. E., and Tsien, R. Y. (2004) *Nat. Biotechnol.* **22,** 1567–1572
40. Fisher, N., Bray, P. G., Ward, S. A., and Biagini, G. A. (2008) *Trends Parasitol.* **24,** 9–10
41. Fisher, N., Warman, A. J., Ward, S. A., and Biagini, G. A. (2009) *Methods Enzymol.* **456,** 303–320
42. Smiley, S. T., Reers, M., Mottola-Hartshorn, C., Lin, M., Chen, A., Smith, T. W., Steele, G. D., Jr., and Chen, L. B. (1991) *Proc. Natl. Acad. Sci. U.S.A.* **88,** 3671–3675
43. Cossarizza, A., Baccarani-Contri, M., Kalashnikova, G., and Franceschi, C. (1993) *Biochem. Biophys. Res. Commun.* **197,** 40–45
44. Raine, J. D., Ecker, A., Mendoza, J., Tewari, R., Stanway, R. R., and Sinden, R. E. (2007) *PLoS Pathog.* **3,** e30
45. Ganter, M., Schüler, H., and Matuschewski, K. (2009) *Mol. Microbiol.* **74,** 1356–1367
46. Hirai, M., and Mori, T. (2010) *Acta Trop.* **114,** 157–161
47. Baker, D. A. (2010) *Mol. Biochem. Parasitol.* **172,** 57–65
48. Vontas, J., Siden-Kiamos, I., Papagiannakis, G., Karras, M., Waters, A. P., and Louis, C. (2005) *Mol. Biochem. Parasitol.* **139,** 1–13
49. Hall, N., Karras, M., Raine, J. D., Carlton, J. M., Kooij, T. W., Berriman, M., Florens, L., Janssen, C. S., Pain, A., Christophides, G. K., James, K., Rutherford, K., Harris, B., Harris, D., Churcher, C., Quail, M. A., Ormond, D., Doggett, J., Trueman, H. E., Mendoza, J., Bidwell, S. L., Rajandream, M. A., Carucci, D. J., Yates, J. R., 3rd, Kafatos, F. C., Janse, C. J., Barrell, B., Turner, C. M., Waters, A. P., and Sinden, R. E. (2005) *Science* **307,** 82–86
50. Terzakis, J. A., Vanderbery, H. P., and Hutter, R. M. (1974) *J. Protozool.* **21,** 251–253
51. Howells, R. E. (1970) *Ann. Trop. Med. Parasitol.* **64,** 181–187
52. Canning, E. U., and Sinden, R. E. (1973) *Parasitology* **67,** 29–40
53. Terzakis, J. A., Sprinz, H., and Ward, R. A. (1967) *J. Cell Biol.* **34,** 311–326
54. Krungkrai, J., Prapunwattana, P., and Krungkrai, S. R. (2000) *Parasite* **7,** 19–26
55. Langreth, S. G., Jensen, J. B., Reese, R. T., and Trager, W. (1978) *J. Protozool.* **25,** 443–452
56. Howells, R. E., Peters, W., and Fullard, J. (1969) *Mil. Med.* **134,** 893–915
57. van Dooren, G. G., Stimmler, L. M., and McFadden, G. I. (2006) *FEMS Microbiol. Rev.* **30,** 596–630
58. Bajohr, L. L., Ma, L., Platte, C., Liesenfeld, O., Tietze, L. F., Gross, U., and Bohne, W. (2010) *Antimicrob. Agents Chemother.* **54,** 517–521
59. Balabaskaran Nina, P., Dudkina, N. V., Kane, L. A., van Eyk, J. E., Boekema, E. J., Mather, M. W., and Vaidya, A. B. (2010) *PLoS Biol.* **8,** e1000418
60. Brown, S. V., Hosking, P., Li, J., and Williams, N. (2006) *Eukaryot. Cell* **5,** 45–53
61. Mogi, T., and Kita, K. (2009) *Mitochondrion* **9,** 443–453
62. Jayabalasingham, B., Bano, N., and Coppens, I. (2010) *Cell Res.* **20,** 1043–1059
63. Mather, M. W., Henry, K. W., and Vaidya, A. B. (2007) *Curr. Drug Targets* **8,** 49–60
64. Ganesan, S. M., Morrisey, J. M., Ke, H., Painter, H. J., Laroiya, K., Phillips, M. A., Rathod, P. K., Mather, M. W., and Vaidya, A. B. (2011) *Mol. Biochem. Parasitol.* **177,** 29–34
65. Carter, V., Shimizu, S., Arai, M., and Dessens, J. T. (2008) *Mol. Microbiol.* **68,** 1560–1569
66. Aikawa, M., and Sterling, C. R. (1974) *Intracellular Parasitic Protozoa*, pp. 1–41, Academic Press, New York